Acta Materialia 231 (2022) 117855

Contents lists available at ScienceDirect

Acta Materialia

journal homepage: www.elsevier.com/locate/actamat

Full length article

Origin of the non-linear elastic behavior of silicate glasses

Zhen Zhang[a,b], Simona Ispas[b], Walter Kob[b,*]

[a] State Key Laboratory for Mechanical Behavior of Materials, Xi'an Jiaotong University, Xi'an 710049, China
[b] Laboratoire Charles Coulomb (L2C), University of Montpellier and CNRS, Montpellier F-34095, France

ARTICLE INFO

Article history:
Received 8 December 2021
Revised 1 March 2022
Accepted 16 March 2022
Available online 26 March 2022

Keywords:
Non-metallic glasses (silicates)
Elastic behavior
Nonlinear
Deformation inhomogeneities
Molecular dynamics simulations

ABSTRACT

For small tension the response of a solid to an applied stress is given by Hooke's law. Outside this linear regime the relation between stress and strain is no longer universal and at present there is no satisfactory insight on how to connect for disordered materials the stress-strain relation to the microscopic properties of the system. Here we use atomistic computer simulations to establish this connection for the case of silicate glasses containing alkali modifiers. By probing how in the highly non-linear regime the stress-strain curve depends on composition, we are able to identify the microscopic mechanisms that are responsible for the complex dependence of stress on strain in these systems, notably the presence of an unexpected quasi-plateau in the tangent modulus. We trace back this dependence to the mobility of the modifiers which, without leaving their cage or modifying the topology of the network, are able to relieve the local stresses. Since the identified mechanism is general, the results obtained in this study will also be helpful for understanding the mechanical response of other disordered materials.

1. Introduction

In contrast to crystalline solids, disordered materials such as oxide glasses, gels etc. have the advantage that their composition can be chosen basically at will, thus allowing for a great flexibility for tuning their mechanical, optical, and electric properties [1–3]. This feature, in combination with the structural isotropy of the material, makes them highly attractive for many applications such as windows panes, optical fibers, polymeric materials, high strength device, food, drugs, micro-devices, etc. The seeked modification of material properties by a change of composition is, however, not always a trivial task since often the relation between composition and property is highly non-linear, as it is, e.g., the case in polymeric systems to which one adds a small amount of plasicizers to enhance the flexibility of the material [3]. This strong dependence is related to the fact that the structural and dynamical properties of disordered systems are influenced by a multitude of competing and counteracting mechanisms, many of which have not yet been understood.

Silicate glasses, arguably the most important class of oxide glasses, are known to have a complex non-linear strain-dependence of the elastic modulus [4–7], which has been shown to be important for questions relating to strength [7–10]. Understanding this non-linear behavior is thus not only of fundamental interest for glass physics but also of importance for the application of these materials, notably in applications under extreme conditions [11–13]. Due to its importance, silica glass has been studied extensively and it has been found that its tangent modulus E_t increases with strain ε up to a maximum at around $\varepsilon = 0.1$ and then decreases again [7,14,15], a behavior that has been termed "anomalous" since most glasses show a decrease of E_t with strain. The maximum of E_t upon tension has been associated with the observation of a maximum in the isothermal compressibility on hydrostatic compression [14,16–19], the origin of which has been attributed to the presence of floppy modes in a mixture of high- and low-density amorphous phases [20].

Many previous studies have focused on the influence of the modifiers on fracture strength and the local atomic defects mediated nanoductility of the glasses [21–24], whereas the origin of the non-linear elastic behavior of modifier-containing glasses, such as alkali silicate, has been investigated much less. It is found that the anomalous properties of silica glass disappear with the addition of modifiers, e.g. Na [13,15]. The transition from anomalous to normal has been attributed to the reduced three-dimension connectivity due to the presence of the network modifiers, although the behavior of these modifiers during deformation has so far not been understood. We also note that previous studies mainly focused on the elastic properties of the glasses at small strains (typically $< 5\%$) [7], whereas the elastic behavior at higher strains (important for applications at extreme conditions) is basically unknown.

* Corresponding author at: Laboratoire Charles Coulomb (L2C), University of Montpellier and CNRS, Montpellier F-34095, France.
E-mail addresses: zhen.zhang@xjtu.edu.cn (Z. Zhang), simona.ispas@umontpellier.fr (S. Ispas), walter.kob@umontpellier.fr (W. Kob).

https://doi.org/10.1016/j.actamat.2022.117855
1359-6454/

The goal of the present work is therefore to probe the highly non-linear regime of the elastic properties of silicate glasses and to identify the relevant mechanisms that give rise to the complex strain and composition dependence of the stress-strain curves of these systems. Importantly, we find that, without changing the topology of the Si–O network, the local variation of the modifier's bonding environment plays a crucial role in determining the nonlinear mechanical response of the glasses. Finally we reveal that the nonlinear elastic behavior of the glasses is manifested on the microscopic scale in the heterogeneous response of the local intertetrahedral linkages.

2. Methods

2.1. Simulation details

The compositions we investigate are pure SiO_2, the binary mixture Na_2O-$xSiO_2$ (NSx) with $x = 3, 5, 10$, and the mixtures A_2O_3-SiO_2 (AS3) with A = Li, Na, K. These systems are of great importance in various fields, such as the glass-making industries and geosciences. Molecular dynamics simulations were performed using a two-body effective potential (SHIK) [25,26] which has been shown to give a reliable description of the structural and mechanical properties of sodium silicate glasses [27,28]. Our samples contain typically 6×10^5 atoms, corresponding to a cubic box of side length around 20 nm, which is sufficiently large to avoid noticeable finite size effects [27]. Periodic boundary conditions were applied in all directions. The samples were first melted and maintained at 3000 K for 800 ps, a time span that is sufficiently long to equilibrate the liquids. (At the end of these equilibration runs the mean squared displacement of Si, i.e. the slowest atomic species, was larger than 100 Å^2 for all samples.) Subsequently, the melts were cooled down to 300 K with a constant cooling rate of 0.25 K/ps. The as-produced glass samples were then annealed at 300 K for 160 ps. All the simulations were carried out in the isothermal-isobaric (NPT) ensemble under zero pressure. Finally, the prepared glass samples were subjected to uniaxial tension with a constant strain rate of 0.5 ns^{-1}. The deformation of the glass was performed in the NPT ensemble, setting the pressure in the directions orthogonal to the strain to zero. We emphasis that the sample size, cooling rate, strain rate, etc. were chosen such that the results presented in this paper do not depend significantly on these parameters (see discussion in Refs. [27,29]). In the Supplementary Materials (Fig. S1) we show that the failure strain, strength and Young's modulus of the simulated glasses are in good agreement with experimental measurements, demonstrating the reliability of our simulations.

Temperature and pressure were controlled using a Nosé-Hoover thermostat and barostat [30–32]. All simulations were carried out using the Large-scale Atomic/Molecular Massively Parallel Simulator software (LAMMPS) [33] with a time step of 1.6 fs. The temperature and pressure damping parameters were chosen to be 0.16 ps and 1.6 ps, respectively. The results presented in the following were obtained from only one melt-quench sample for each composition but we emphasize that the system sizes considered in this study are sufficiently large to make sample-to-sample fluctuations negligible as long as the samples do not start to fracture. The error bars were estimated as the standard deviation from 3 simulations in which the samples were put under tension in the 3 different axial directions.

2.2. Bonding environment of the modifiers

The modifiers' behavior was investigated by analyzing the change of their bonding environment during deformation. The bonding environment of a given modifier atom was determined by identifying, at a given strain, the oxygen neighbors in its first coordination shell, which is defined by the minimum between the first and second peaks in the radial distribution function of alkali-oxygen. We then calculated the probability that a modifier changes this bonding environment by comparing two adjacent configurations separated 1% strain.

2.3. Vibrational displacement of the atoms

Below we will see that it is useful to study the vibrational motion of the atoms. To characterize this local motion of the atoms as a function of the deformation, we take the configuration corresponding to a given strain and then performed a simulation at 300 K in the NVT ensemble (constant volume and temperature) for several tens of picoseconds. From this simulation, the displacements of the atoms were monitored. We then measured the size of the cage of local atomic vibration using the vibrational displacement which is defined as $\lambda_i = \sqrt{\langle [\vec{r}_i(t) - \vec{r}_i(0)]^2 \rangle_{\tau_0}}$, where $\vec{r}_i(t)$ is the position of atom i at time t and τ_0 is the time interval over which we take the average of the atomic displacement. We have chosen τ_0 to be 0.4–0.5 ps since this time scale corresponds to the appearance of the plateau in the mean-squared displacement (MSD), see Fig. S2 in the Supplementary Materials.

3. Results and discussion

Fig. 1 presents the macroscopic stress-strain (SS) curves and their derivatives, i.e., the tangent modulus E_t of the glasses. From panel (a) one recognizes that the addition of Na_2O to the SiO_2 glass leads to a decrease of the strength, i.e., the maximum attainable stress before failure, and an increase of the ductility, i.e., the ability of a material to elongate under tensile loading. Also, the decreasing slope of the SS curve with the addition of Na shows that the presence of the network modifiers softens the network at large strains.

In panel (b) the influence of the modifier on the mechanical properties is quantified and one recognizes that already at $\varepsilon = 0$ the addition of 25% Na_2O reduces the Young's modulus of the glass from around 71 GPa for silica to 56 GPa for NS3, in good agreement with experimental findings [35–37]. This softening of the glass is mainly due to the decrease in network connectivity as the concentration of modifiers increases [38]. Other concurrent factors, including the enhanced cohesion of the glass by the formation of new alkali-NBO bonds and the decreased free volume, can also be relevant but, for the case of sodium silicate glasses, play only a minor role [39]. From this graph one also recognizes that the non-linear elastic behavior of the glasses can roughly be divided into three regimes, each of which has a different strain dependence of E_t, marked by the two arrows which indicate the two strains ε_1 and ε_2 that delimit these regions. In Fig. 1(c) we show the derivative of E_t and one sees that for all the considered glasses with sodium this function has a clear minimum, followed by a maximum. The strain at the mid-point between these minima/maxima can thus be used to define ε_1, marked by circles in the graph, and the strain ε_2, marked by squares, at which the function is zero (before the final decay upon approaching the failure point). For $\varepsilon < \varepsilon_1$ the addition of Na makes that $E_t(\varepsilon)$ gradually transform from anomalous (i.e. E_t increases) to intermediate (E_t remains almost constant) and finally to normal (E_t decreases), in agreement with experimental findings [5,7]. In the second regime, i.e., $\varepsilon_1 < \varepsilon < \varepsilon_2$, one finds for the Na-rich glasses, NS5 and NS3, that E_t is basically independent of strain. This result is surprising since naively one anticipates a continuous softening of the glass upon increasing strain. In order to ensure that this finding is not just a particularity of the interaction potential, we have also calculated E_t using other popular potentials [40,41] (although computa-

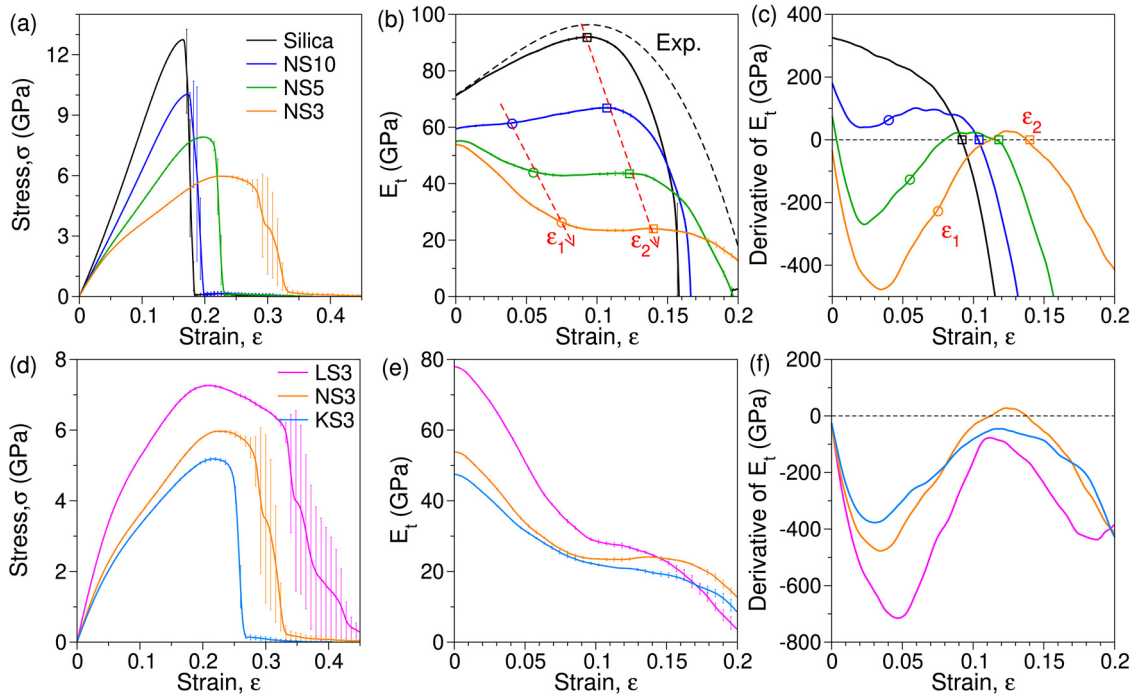

Fig. 1. (a) and (b) are, respectively, the stress-strain curves and the corresponding tangent modulus E_t for the NSx glasses. The black dashed curve in (b) is the fit to experimental data of silica glass fibers up to 7% strain [34]. The red dashed lines are a guide to the eye, highlighting two characteristic strains, ε_1 and ε_2, which are indicated by the symbols. (c): Derivative of E_t. The circles and squares show the location of ε_1 and ε_2, respectively. See main text for details. (d)–(f) are the corresponding curves for the AS3 glasses. All three compositions show a bend in their tangent modulus at $\varepsilon \approx 0.08$ but this feature is most pronounced for NS3. (For interpretation of the references to color in this figure legend, the reader is referred to the web version of this article.)

tionally more expensive) and the results (see Fig. S3) show that the observed plateau in E_t for the Na-rich glasses is a robust feature. If the Na concentration is lowered, the ε-dependence of E_t in this second regime becomes also anomalous, although the slope of E_t is different from the one at small strains, from which we conclude that the mentioned plateau is related to the high concentration of network modifiers. For the third regime, $\varepsilon > \varepsilon_2$, all the E_t curves show a rapid decrease which can be attributed to global yielding of the glasses.

Fig. 1 (d) and (e) show the SS and the resulting E_t curves for the different AS3 glasses. From panel (d) one recognizes that the glasses with small alkali atoms have not only higher strength but they are also more ductile. Thus reducing the size of the modifiers is a viable strategy to improve the toughness of the glass, in accordance with experimental findings [42]. From Fig. 1(e) one recognizes that the Young's modulus of the glasses follows the order LS3 > NS3 > KS3 and in Fig. S1(e) we demonstrate that our results agree well with the experimental values. The dependence of the Young's modulus on the alkali type has been discussed by Pedone et al. [39] who showed that Li can act as a pseudo-network former with four-fold coordination and a large force constant, thus promoting the cross-linking and cohesion of the network. In comparison to Li, Na and K have higher coordination numbers and smaller force constants and hence they act primarily as network modifiers which depolymerize the network and lead to a reduced Young's modulus. More important for the subject of the present study is the fact that also LS3 and KS3 exhibit a similar ε-dependence of E_t and its derivative, panel (f), as observed for NS3. This indicates that the unexpected non-linear ε-dependence of E_t is universal for alkali-containing glasses, hinting a common origin and in the following we will identify the microscopic mechanism leading to this behavior.

Usually the network topology (NT) is a convenient structural observable for understanding the mechanical behavior of

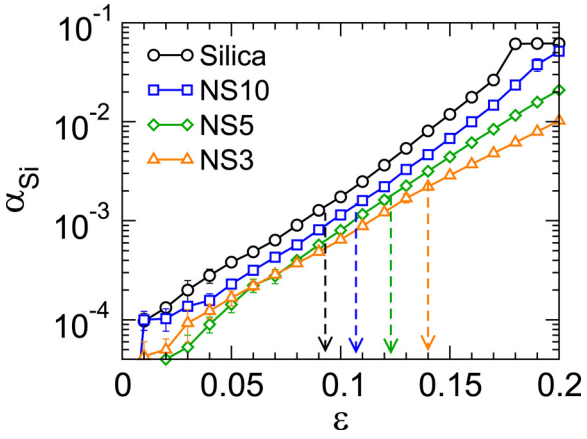

Fig. 2. Fraction of Si atoms that have changed their bonding environment, see main text for definition. The vertical arrows from left to right indicate approximately the ε_2 of silica, NS10, NS5, and NS3, respectively.

glasses [43–45] and therefore we investigate its dependence on strain. Here we characterize the change of the NT by mean of $\alpha_{\mathrm{Si}}(\varepsilon)$, the fraction of Si atoms that have changed their bonding partners if the strain is increased from zero to ε, i.e. $\alpha_{\mathrm{Si}} = N'_{\mathrm{Si}}/N_{\mathrm{Si}}$, where N'_{Si} is the number of Si atoms which have at least one of their neighbors changed with respect to the configuration at $\varepsilon = 0$ and N_{Si} is the total number of Si atoms. Fig. 2 shows that α_{Si} is small for all relevant strains, demonstrating that the bonding environment of all network atoms is basically unchanged ($\alpha_{\mathrm{Si}} < 0.3\%$ up to ε_2). In other words, the Si–O network remains basically intact during tension up to intermediate strains, a result that is also found for the glasses with Li or K, see Fig. S7. Hence we conclude

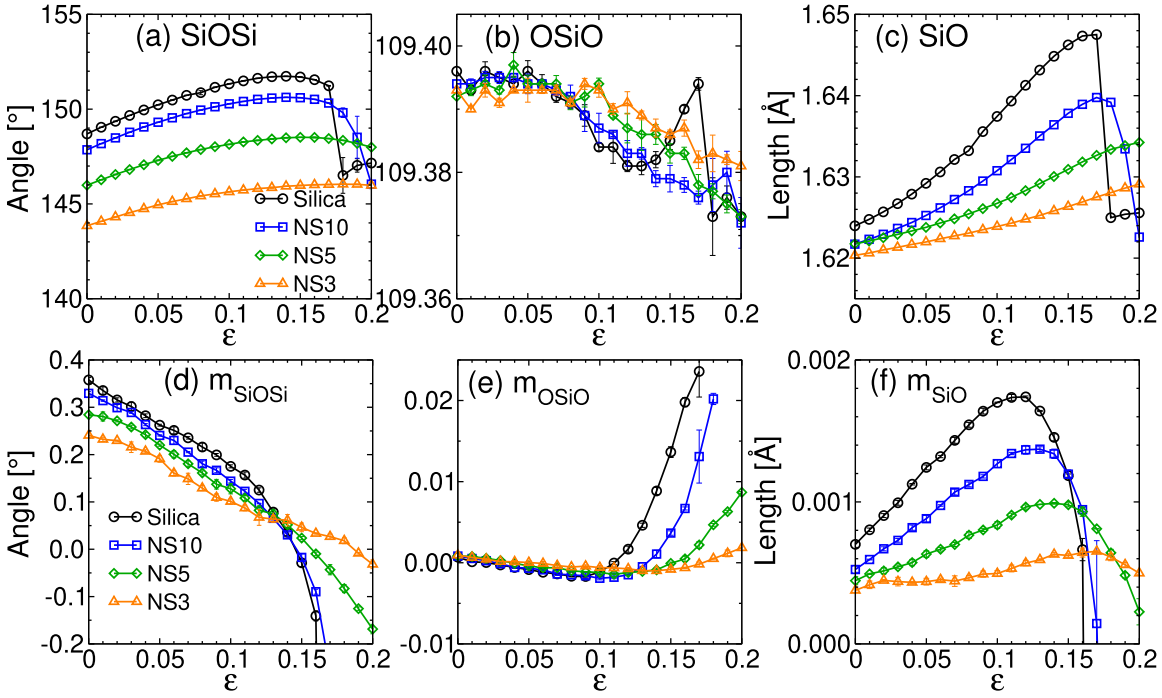

Fig. 3. Structural quantities that characterize various deformation modes of the Si–O network. (a)–(c): The mean values. (d)–(f): The corresponding derivatives.

that the decrease of E_t with strain is not due to a changing topology of the SiO network.

Since the deformation of the sample is not accompanied by a relevant modification of the NT, one can conclude that on the atomic scale this deformation must be due to: 1) the distortion of the tetrahedral units, which can be characterized by the change in SiO bond length and the intra-tetrahedral OSiO angle; 2) rotation of the tetrahedra (assuming that the tetrahedra are rigid bodies); 3) bending motion of the inter-tetrahedral linkages (characterized by the SiOSi angle). We note that although in theory the three forms of deformation can be independent of each other, in practice they are intimately related. One expects that the coupling between (2) and (3) is stronger than the ones between (1) and (2) or (3) since changing the shape of the tetrahedral units is energetically more expensive than the rotation or bending motions and below we will show that this is indeed the case.

In order to identify the relevant type of deformation we investigate in the following the related structural quantities as well as their derivatives with respect to strain. Fig. 3(a)–(c) demonstrate that the change of the OSiO angle and SiO bond length is much weaker that the one of the SiOSi angle which indicates that the deformation of the sample is mainly due to the change of the inter-tetrahedral linkages. Surprisingly we find that none of the quantities presented in Fig. 3(a)–(c) show an ε-dependence that mirrors the one of E_t, indicating that these quantities are not the relevant ones for rationalizing the strain dependence of E_t. However, since E_t represents the slope of the SS curve, one has also to check whether $E_t(\varepsilon)$ is related to the *derivative* of the structural quantities. Fig. 3(d)–(f) show that the slope $m_X = dX/d\varepsilon$ does not match the ε-dependence of E_t. (Fig. S8 shows that this observation is independent of the nature of the modifiers.) This absence of a correlation between structural quantities and E_t can be rationalized by recalling that E_t is an observable that describes the global response of the system while the considered structural observables X are local quantities and hence the strain dependence of their average does not necessarily reflect the one of the macroscopic behavior. For example, the insertion of a soft link in a one-dimensional chain will weaken the whole system although the average bond strength is still high. Below we will discuss these mechanical heterogeneities in more detail.

Since neither the change of the NT nor the local structural quantities associated with the SiO network are able to rationalize the strain dependence of E_t we turn our attention to the network modifiers. For this it is instructive to imagine a separation of the mechanical responses into a contribution from the bare Si–O network (i.e. assuming absence of the modifiers) and one from the modifiers. For the case of silica, we have seen that the network rigidity, as characterized by E_t, increases with strain if $\varepsilon < \varepsilon_2$. It is therefore reasonable to assume that this rigidity will always increase with strain, regardless of the network connectivity. However, the slope of $E_t(\varepsilon)$ of the network will depend on the modifier content since the SiO network is increasingly deteriorated by the addition of modifiers, thus making it more flexible. This idea is schematically illustrated in Fig. 4(a) by the two dashed lines, along with the two solid lines that represent the real response of the glasses including the effect of modifiers. A crucial step is thus to identify the microscopic mechanism which transforms the dashed lines to the solid ones.

Since the Si–O bonding environment is basically unchanged upon applied tension (Fig. 2), the only way the sample can acquire additional deformability is via the motion of the Na atoms since these are weakly bonded to the SiO network and hence are mobile [46]. In the following we focus on the NSx glasses for elucidating the role of the modifiers. By analyzing the coordination of the Na atoms, we find that these modifiers are indeed changing their local environment during the deformation via bond switching, a phenomenon that has been proposed to be responsible for the plasticity in other amorphous materials [47–51]. (Fig. S10 shows that the coordination number (Z) and nearest neighbors of Na depend strongly on strain). More specifically, a Na atom can change its bonding by swapping bonds leaving Z unchanged, by increasing Z, or by decreasing Z, see the snapshots in Fig. 4(c). It is thus useful to quantify the intensity of such bond switching events (BSEs)

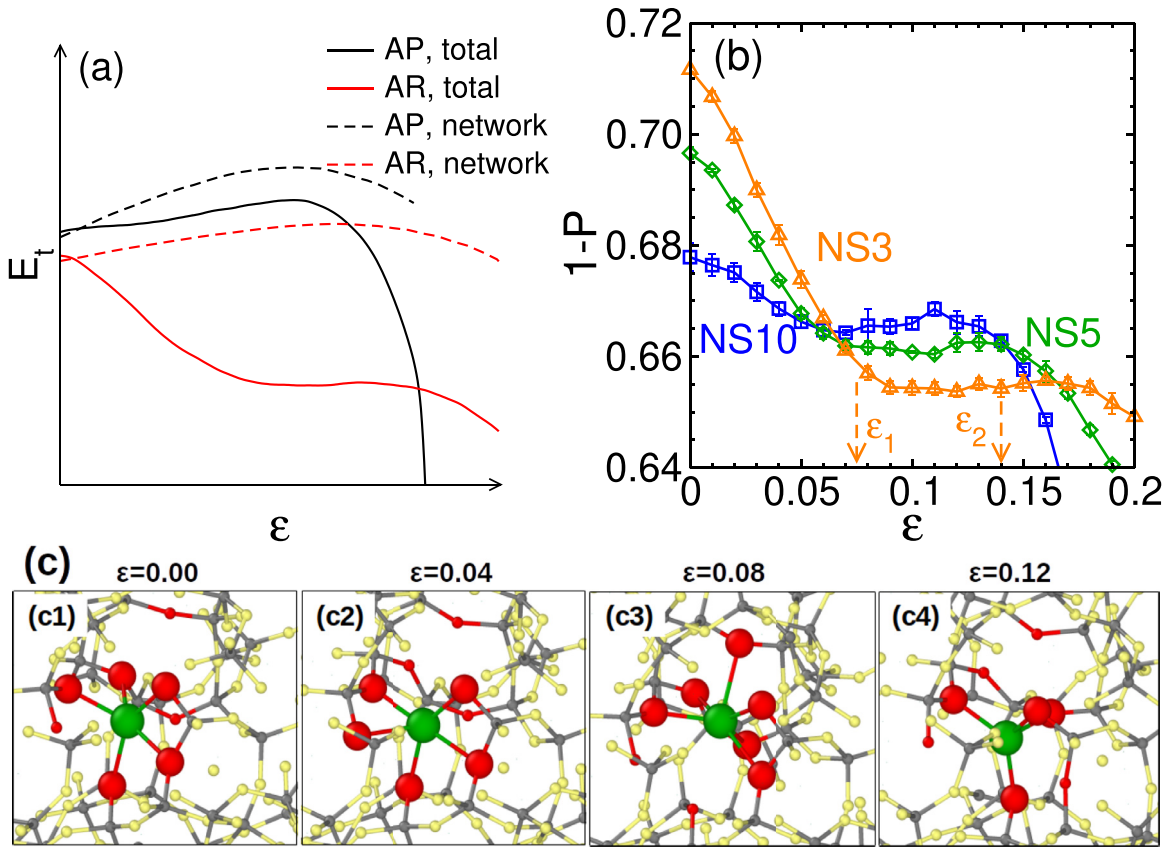

Fig. 4. (a): Sketch of the strain-dependence of E_t for an alkali-poor (AP) and an alkali-rich (AR) glass. The solid and dashed curves represent the responses of the whole sample and the SiO network alone, respectively. (b): Probability that a Na atom will not change its bonding environment if the strain is increased by 1%, see main text for definition. The two dashed lines indicate ε_1 and ε_2 for the NS3 glass. (c1)–(c4): Snapshots showing the change of bonding environment of a Na atom during the deformation of NS3. From left to right: $\varepsilon = 0.00$, 0.04, 0.08, and 0.12. (c2)–(c4) present, respectively, the three possibilities for a change in the bonding of the reference Na: Unchanged Z but swapped bond, increasing Z, and decreasing Z. The atom colors depict Na (green), Si (grey), O (red and yellow). The O atoms that are currently bonded to the Na are colored red and enlarged for clarity. The bond lengths are smaller than the distances corresponding to the first minimum in $g_{\mathrm{NaO}}(r)$ and $g_{\mathrm{SiO}}(r)$. (For interpretation of the references to color in this figure legend, the reader is referred to the web version of this article.)

in a given sample by the probability P that a Na atom changes its bonding per unit change of ε.

For a better comparison with the data shown in panel (a), we show in panel (b) $1-P$, i.e., the probability that a Na atom is not going to change its bonding environment if strain is increased by 1%. Interestingly, this quantity shows a non-trivial ε-dependence with three distinct stages that are delimited by ε_1 and ε_2, i.e., at the same critical strains observed for E_t. Also remarkable is that the height of the plateau at intermediate strain depends only weakly on the concentration of the Na atoms, which indicates that collective effects are not important for this motion. The solid curves in panel (a) can thus be rationalized by postulating that the total response of the structure is given by the sum of the response of the SiO network (i.e. the dashed lines in panel (a)) and of the modifiers (i.e. the curves in panel (b)). The dependence of $E_t(\varepsilon)$ on the Na concentration can hence be attributed to the increasing influence of the Na atoms that switch bonds and thus release the local stress, leading to the presence of the plateau in E_t if the modifier concentration is sufficiently large.

Figure S11 in the Supplementary Materials shows that the bond switching probability depends strongly on the type of modifier in that P increases with the size of the alkali atom. This increase of P with alkali size can be related to the fact that atoms with larger size have a higher coordination number Z which makes the change of bonding environment more probable. (See Fig. S12 for the ε-dependence of Z for the three types modifiers). This simple effect and the arguments presented above for the softening of the structure as a function of P provide thus a microscopic explanation for the observation that E_t reduces with increasing alkali size, see Fig. 1(d). However, it should be noted that although Fig. 4(b) gives strong evidence that the bond switching mechanism is a key ingredient for understanding the non-linear elastic behavior of the modifier-containing glasses, it is likely not to be the only one that gives rise to ductility in the material, especially when the strain is large (say after the maximum strength) and non-local plastic deformation modes also become active. The fact that LS3 is more ductile than NS3 and KS3 (Fig. 1d) might be related to the fact that LS3 has a more cross-linked network [39], which allows for a more uniform deformation before strain localization (necking).

In Fig. 4(b) the rapid decrease of $1-P$, i.e., the intensity of the BSEs increases, at large strains ($\varepsilon > \varepsilon_2$) reflects simply the yielding of the glass structure on the global scale. In contrast to this, the plateau in the ε-dependence of P is surprising and its origin needs to be clarified. Since we have seen that the BSEs are due to the motion of the alkali atoms and not of the network, it is useful to probe their motion in more detail. Figure S13 demonstrates that during the tension most of the Na atoms move only by a small distance, i.e., have a small non-affine displacement, and that the probability for a Na atom to escape from its cage occupied at $\varepsilon = 0$ is at most a few percent up to the critical strain ε_2. Thus it is reasonable to view the BSEs as discussed above to be basically of vibrational nature. We have therefore determined the mean vibra-

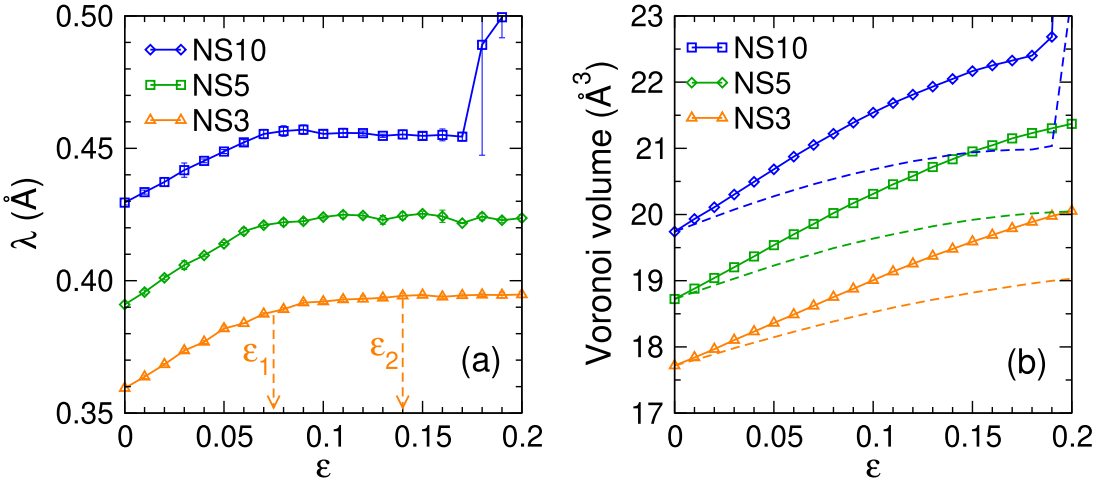

Fig. 5. (a) Mean vibration displacement of the Na atoms, see the main text for definition. The dashed lines indicate ε_1 and ε_2 for NS3. (b) Atomic volume of Na estimated by Voronoi tessellation. The dashed lines are for affine deformation.

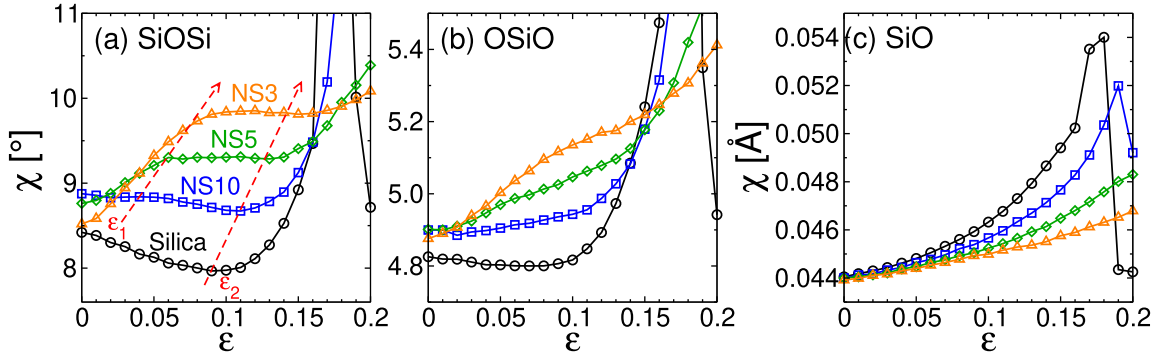

Fig. 6. Standard deviation of the incremental structural quantities. (a): SiOSi angle; (b) OSiO angle; (c) SiO bond length. In panel (a), ε_1 and ε_2 are indicated by arrows.

tional displacement λ of the modifier atoms which is proportional to the size of the cage within which the atoms vibrate locally (see Section 2.3).

Fig. 5 (a) shows that λ first increases before saturating at a value of the strain that is close to ε_1. This saturation is rather surprising since the locally available space for the Na atoms, characterized by their Voronoi volume, increases monotonously with strain, see panel (b). (This increase is directly related to the fact that for these glasses the Poisson's ratio is smaller than 0.5, see Fig. S14.) Hence we conclude that for $\varepsilon < \varepsilon_1$ the increasing atomic volume allows the Na atoms to vibrate with a larger amplitude but that above a certain volume this amplitude has reached its maximum value. This increasing amplitude allows the Na atom to change bonding partners and therefore λ shows a similar ε-dependence as P, see Fig. 4(b), which in turn leads to the decrease of E_t. Once the maximum amplitude is reached, the intensity of the BSEs becomes independent of ε, and together with the weak ε-dependence of the network rigidity (Fig. 4(a)), E_t becomes nearly a constant.

In the context of Fig. 3 we have argued that the plateau in E_t is not seen in the mean value of the structural quantities because the mechanical response will be strongly influenced by the structural heterogeneities of the sample. To probe the effect of these heterogeneities we determine how a local structural quantity X (angle, bond length, etc.) changes per unit change of ε, giving ΔX. We find that for all cases considered, the distribution of ΔX is described well by a Gaussian, see Fig. S9, and therefore its standard deviation χ_X is a good measure of the heterogeneity of the response of the system.

In Fig. 6 we present χ_X for different quantities X. Remarkably, one sees that the ε-dependence of χ_{SiOSi}, panel (a), matches very well the one of the E_t, i.e. a nearly perfect anti-correlation between the two quantities is observed, irrespective of the composition. (Figure S8 shows that this good correspondence is unaffected by changing the alkali species.) For silica, the network is fully connected and becomes increasingly rigid with strain (E_t increases) and this is accompanied by a decrease of χ_{SiOSi}, i.e. the system becomes more homogeneous. However, the stiffening of the network reaches a limit at around 10% strain, beyond which the structure will yield globally. Consequently, with further increasing strain the structure softens, E_t decreases, and χ_{SiOSi} increases quickly. Also the strain-dependence of χ_{SiOSi} for alkali silicate glasses can be rationalized in terms of the responses of the Si–O network and of the modifiers: On one hand, the response of the Si–O network becomes more homogeneous with strain (as it is the case for pure silica), thus decreasing χ_{SiOSi}, and on the other hand the modifiers will move more if the local stress is high (i.e., strong deviations of the SiOSi angle from its mean) and hence this local motion and the associated bond switching events tend to make the mechanical response of the glass more heterogeneous, thus increasing χ_{SiOSi}. The sum of the two effects allows thus to rationalize how χ_{SiOSi} depends on strain and the Na concentration.

It is also interesting to examine the values of χ_{SiOSi} at $\varepsilon = 0$. Starting from silica one finds that a small addition of modifiers makes the structural response more heterogeneous (the case of NS10). However, further addition of modifiers tend to homogenize again this response (the case of NS5 and NS3), i.e., χ_{SiOSi} decreases again. Thus χ_{SiOSi} can be used directly to probe the importance

of the heterogeneities. This data also demonstrates that a small χ_{SiOSi} is not necessarily associated with a large E_t. This can be rationalized by the fact that E_t is related not only to the heterogeneous response of the local structure but also to the overall three-dimensional connectivity of the network which depends strongly on the composition.

From Fig. 6(b) one sees that χ_{OSiO} shows the same qualitatively ε-dependence as χ_{SiOSi}. However, the relative change of χ_{OSiO} is significantly smaller than the one found in χ_{SiOSi}, indicating that the ε-dependence of the heterogeneity in the OSiO angular response is mainly due to the coupling of this angle with the SiOSi angle. The ε-dependence of χ_{SiO}, panel (c), is qualitatively very different from the ones for the angles in that the heterogeneity increases monotonously for all compositions, indicating that this quantity is not relevant for the dependence of the flexibility of the network on composition. These results support our argument made above that the distortion of the tetrahedra is energetically costly compared to other deformation modes, in agreement with the fact that in the vibrational density of states intra-tetrahedral vibrational modes (mainly stretching) are at higher frequencies than the inter-tetrahedral ones (bending and rocking) [52]. We thus have strong evidence that the heterogeneous response of the inter-tetrahedral linkages, influenced by the unusual dynamical behavior of the modifiers, is the primary structural manifestation of the non-linear elastic properties of the glasses.

4. Conclusions

We have demonstrated that for the case of silicate glasses the presence of heterogeneities in the local structural properties gives rise to an unexpected behavior of the non-linear elastic behavior of such systems. This behavior is intimately related to the presence of species (here the alkali atoms) that are more mobile than the atoms forming the matrix (SiO network) since they allow to react locally to the applied stress. Although we are not aware of any experimental results regarding this unexpected mechanical behavior, its detection should be possible by carefully probing the elastic properties of alkali-silicate glasses at large tensile strains. While previous studies have shown that the nature of the alkali ions influences strongly the structure and the elastic properties of the glasses [39], our results suggest that the mechanism which is responsible for the non-linear elastic behavior of the alkali silicate glasses is very general, i.e. independent of the alkali type. Note that although the details regarding the decoupling of the response between mobile and immobile parts of the sample will depend on the system considered, it can be expected that the identified mechanism is in fact very general for materials which consist of atomic species with distinctive mobilities. Our findings can thus be expected to trigger further studies on the deformation behavior of complex materials and should also be of practical relevance for the design of materials with tailored mechanical properties.

Data availability

All data needed to evaluate the conclusions in the paper are present in the paper and/or the Supplementary Materials. Additional data related to this paper may be requested from the authors.

Declaration of Competing Interest

The authors declare that they have no known competing financial interests or personal relationships that could have appeared to influence the work reported in this paper.

Acknowledgments

We thank P. K. Gupta for discussions. ZZ acknowledges a grant from China Scholarship Council (No. 201606050112). WK is member of the Institut Universitaire de France. The simulations were done by utilizing the HPC resources of CINES under the allocation A0050907572 and A0070907572 attributed by GENCI (Grand Equipement National de Calcul Intensif) and the computational resources at XJTU.

Supplementary material

Supplementary material associated with this article can be found, in the online version, at doi:10.1016/j.actamat.2022.117855.

References

[1] K. Binder, W. Kob, Glassy Materials and Disordered Solids: An Introduction to Their Statistical Mechanics, World Scientific, 2011.
[2] A.K. Varshneya, J. Mauro, Fundamentals of Inorganic Glasses, Elsevier, 2019.
[3] M.K. Rubinstein, R. Colby, Polymer Physics, Oxford University Press, 2003.
[4] F.P. Mallinder, B.A. Proctor, Elastic constants of fused silica as a function of large tensile strain, Phys. Chem. Glasses 5 (4) (1964) 91–103.
[5] J.T. Krause, L.R. Testardi, R.N. Thurston, Deviations from linearity in the dependence of elongation on force for fibers of simple glass formers and of glass optical lightguides, Phys. Chem. Glasses 20 (6) (1979) 135–399.
[6] C.R. Kurkjian, Strength of Inorganic Glass, Plenum Press, 1985.
[7] P.K. Gupta, C.R. Kurkjian, Intrinsic failure and non-linear elastic behavior of glasses, J. Non-Cryst. Solids 351 (27–29) (2005) 2324–2328, doi:10.1016/j.jnoncrysol.2005.05.029.
[8] C.R. Kurkjian, P.K. Gupta, R.K. Brow, The strength of silicate glasses: what do we know, what do we need to know? Int. J. Appl. Glass Sci. 1 (1) (2010) 27–37.
[9] L. Wondraczek, J.C. Mauro, J. Eckert, U. Kühn, J. Horbach, J. Deubener, T. Rouxel, Towards ultrastrong glasses, Adv. Mater. 23 (39) (2011) 4578–4586, doi:10.1002/adma.201102795.
[10] L.A. Mihai, A. Goriely, How to characterize a nonlinear elastic material? Areview on nonlinear constitutive parameters in isotropic finite elasticity, Proc. R. Soc. A 473 (2207) (2017) 20170607.
[11] E. Suhir, Elastic stability, free vibrations, and bending of optical glass fibers: effect of the nonlinear stress–strain relationship, Appl. Opt. 31 (24) (1992) 5080–5085.
[12] F.T. Wallenberger, Commercial and experimental glass fibers, Fiberglass Glass Technol. (2010) 3–90.
[13] S.M. Wiederhorn, H. Johnson, A.M. Diness, A.H. Heuer, Fracture of glass in vacuum, J. Am. Ceram. Soc. 57 (8) (1974) 336–341, doi:10.1111/j.1151-2916.1974.tb10917.x.
[14] A. Pedone, G. Malavasi, M.C. Menziani, U. Segre, A.N. Cormack, Molecular dynamics studies of stress-strain behavior of silica glass under a tensile load, Chem. Mater. 20 (13) (2008) 4356–4366, doi:10.1021/cm800413v.
[15] F. Yuan, L. Huang, Molecular dynamics simulation of amorphous silica under uniaxial tension: from bulk to nanowire, J. Non-Cryst. Solids 358 (24) (2012) 3481–3487, doi:10.1016/j.jnoncrysol.2012.05.045.
[16] P.W. Bridgman, The compressibility of several artificial and natural glasses, Am. J. Sci. 10 (58) (1925) 359–367, doi:10.2475/ajs.s5-10.58.359.
[17] P.W. Bridgman, The high pressure behavior of miscellaneous minerals, Am. J. Sci. 237 (1) (1938) 7–18, doi:10.2475/ajs.237.1.7.
[18] C. Meade, R. Jeanloz, Frequency-dependent equation of state of fused silica to 10 GPa, Phys. Rev. B 35 (1) (1987) 236.
[19] O. Tsiok, V. Brazhkin, A. Lyapin, L. Khvostantsev, Logarithmic kinetics of the amorphous-amorphous transformations in SiO_2 and GeO_2 glasses under high pressure, Phys. Rev. Lett. 80 (5) (1998) 999.
[20] A.N. Clark, C.E. Lesher, S.D. Jacobsen, S. Sen, Mechanisms of anomalous compressibility of vitreous silica, Phys. Rev. B 90 (17) (2014) 174110, doi:10.1103/PhysRevB.90.174110.
[21] T.F. Soules, R.F. Busbey, The rheological properties and fracture of a molecular dynamic simulation of sodium silicate glass, J. Chem. Phys. 78 (10) (1983) 6307–6316, doi:10.1063/1.444556.
[22] A. Pedone, M.C. Menziani, A.N. Cormack, Dynamics of fracture in silica and soda-silicate glasses: from bulk materials to nanowires, J. Phys. Chem. C 119 (45) (2015) 25499–25507, doi:10.1021/acs.jpcc.5b08657.
[23] B. Wang, Y. Yu, Y.J. Lee, M. Bauchy, Intrinsic nano-ductility of glasses: the critical role of composition, Front. Mater. 2 (2015) 11, doi:10.3389/fmats.2015.00011.
[24] B. Wang, Y. Yu, M. Wang, J.C. Mauro, M. Bauchy, Nanoductility in silicate glasses is driven by topological heterogeneity, Phys. Rev. B 93 (6) (2016) 064202.
[25] S. Sundararaman, L. Huang, S. Ispas, W. Kob, New optimization scheme to obtain interaction potentials for oxide glasses, J. Chem. Phys. 148 (19) (2018) 194504, doi:10.1063/1.5023707.
[26] S. Sundararaman, L. Huang, S. Ispas, W. Kob, New interaction potentials for alkali and alkaline-earth aluminosilicate glasses, J. Chem. Phys. 150 (15) (2019) 154505, doi:10.1063/1.5079663.

[27] Z. Zhang, S. Ispas, W. Kob, The critical role of the interaction potential and simulation protocol for the structural and mechanical properties of sodosilicate glasses, J. Non-Cryst. Solids 632 (2020) 119895.
[28] Z. Zhang, S. Ispas, W. Kob, Structure and vibrational properties of sodium silicate glass surfaces, J. Chem. Phys. 153 (12) (2020) 124503.
[29] Z. Zhang, Fracture, Surface, and Structure of Silicate Glasses: Insights from Atomistic Computer Simulations, University of Montpellier, 2020 Doctoral dissertation.
[30] S. Nosé, A unified formulation of the constant temperature molecular dynamics methods, J. Chem. Phys. 81 (1) (1984) 511–519, doi:10.1063/1.447334.
[31] W.G. Hoover, Canonical dynamics: equilibrium phase-space distributions, Phys. Rev. A 31 (3) (1985) 1695–1697, doi:10.1103/PhysRevA.31.1695.
[32] W.G. Hoover, Constant-pressure equations of motion, Phys. Rev. A 34 (3) (1986) 2499–2500, doi:10.1103/PhysRevA.34.2499.
[33] S. Plimpton, Fast parallel algorithms for short-range molecular dynamics, J. Comput. Phys. 117 (1) (1995) 1–19.
[34] M. Guerette, C.R. Kurkjian, S. Semjonov, L. Huang, Nonlinear elasticity of silica glass, J. Am. Ceram. Soc. 99 (3) (2016) 841–848, doi:10.1111/jace.14043.
[35] N.P. Bansal, R.H. Doremus, Handbook of Glass Properties, Academic Press, Orlando, 1986.
[36] N.P. Lower, R.K. Brow, C.R. Kurkjian, Inert failure strain studies of sodium silicate glass fibers, J. Non-Cryst. Solids 349 (2004) 168–172.
[37] K. Januchta, T. To, M.S. Bødker, T. Rouxel, M.M. Smedskjaer, Elasticity, hardness, and fracture toughness of sodium aluminoborosilicate glasses, J. Am. Ceram. Soc. 102 (8) (2019) 4520–4537, doi:10.1111/jace.16304.
[38] T. Rouxel, Elastic properties and short-to medium-range order in glasses, J. Am. Ceram. Soc. 90 (10) (2007) 3019–3039, doi:10.1111/j.1551-2916.2007.01945.x.
[39] A. Pedone, G. Malavasi, A.N. Cormack, U. Segre, M.C. Menziani, Insight into elastic properties of binary alkali silicate glasses; prediction and interpretation through atomistic simulation techniques, Chem. Mater. 19 (13) (2007) 3144–3154, doi:10.1021/cm062619r.
[40] J. Habasaki, I. Okada, Molecular dynamics simulation of alkali silicates based on the quantum mechanical potential surfaces, Mol. Simul. 9 (5) (1992) 319–326.
[41] S.H. Hahn, J. Rimsza, L. Criscenti, W. Sun, L. Deng, J. Du, T. Liang, S.B. Sinnott, A.C.T. van Duin, Development of a ReaxFF reactive force field for $NaSiO_X$/water systems and its application to sodium and proton self-diffusion, J. Phys. Chem. C 122 (34) (2018) 19613–19624, doi:10.1021/acs.jpcc.8b05852.
[42] C.R. Kurkjian, P.K. Gupta, Intrinsic strength and the structure of glass, in: Proc. Int. Congr, 2001, pp. 11–18.
[43] J.C. Mauro, Topological constraint theory of glass, Am. Ceram. Soc. Bull. 90 (4) (2011) 31.
[44] M. Bauchy, Deciphering the atomic genome of glasses by topological constraint theory and molecular dynamics: a review, Comput. Mater. Sci 159 (2019) 95–102.
[45] Q. Zheng, H. Zeng, Progress in modeling of glass properties using topological constraint theory, Int. J. Appl. Glass Sci. 11 (2020) 432–441.
[46] J. Horbach, W. Kob, K. Binder, Dynamics of sodium in sodium disilicate: channel relaxation and sodium diffusion, Phys. Rev. Lett. 88 (12) (2002) 125502, doi:10.1103/PhysRevLett.88.125502.
[47] K. Zheng, C. Wang, Y.-Q. Cheng, Y. Yue, X. Han, Z. Zhang, Z. Shan, S.X. Mao, M. Ye, Y. Yin, E. Ma, Electron-beam-assisted superplastic shaping of nanoscale amorphous silica, Nat. Commun. 1 (1) (2010) 24, doi:10.1038/ncomms1021.
[48] J. Luo, J. Wang, E. Bitzek, J.Y. Huang, H. Zheng, L. Tong, Q. Yang, J. Li, S.X. Mao, Size-dependent brittle-to-ductile transition in silica glass nanofibers, Nano Lett. 16 (1) (2016) 105–113, doi:10.1021/acs.nanolett.5b03070.
[49] E.J. Frankberg, J. Kalikka, F.G. Ferré, L. Joly-Pottuz, T. Salminen, J. Hintikka, M. Hokka, S. Koneti, T. Douillard, B.L. Saint, P. Kreiml, M.J. Cordill, T. Epicier, D. Stauffer, M. Vanazzi, L. Roiban, J. Akola, F.D. Fonzo, E. Levänen, K. Masenelli-Varlot, Highly ductile amorphous oxide at room temperature and high strain rate, Science 366 (6467) (2019) 864–869, doi:10.1126/science.aav1254.
[50] K. Lee, Y. Yang, L. Ding, B. Ziebarth, M.J. Davis, J.C. Mauro, Plasticity of borosilicate glasses under uniaxial tension, J. Am. Ceram. Soc. 103 (8) (2020) 4295–4303, doi:10.1111/jace.17163.
[51] T. To, S.S. Sørensen, J.F. Christensen, R. Christensen, L.R. Jensen, M. Bockowski, M. Bauchy, M.M. Smedskjaer, Bond switching in densified oxide glass enables record-high fracture toughness, ACS Appl. Mater. Interfaces 13 (15) (2021) 17753–17765.
[52] S.N. Taraskin, S.R. Elliott, Nature of vibrational excitations in vitreous silica, Phys. Rev. B 56 (14) (1997) 8605–8622, doi:10.1103/PhysRevB.56.8605.